Vacuum-Field Catalysis: Accelerated Reactions by Vibrational Ultra Strong Coupling

Hidefumi Hiura[1*] & Atef Shalabney[2]

[1]System Platform Research Laboratories, NEC Corporation, 34 Miyukigaoka, Tsukuba 305-8501, Japan

[2]Physics and Optical Engineering Department, Braude College, Snunit St 51, Karmiel, 2161002 Israel

In conventional catalysis, the reactants interact with specific sites of the catalyst in such a way that the reaction barrier is lowered by changing the reaction path, causing the reaction rate to be accelerated. Here we take a radically different approach to catalysis by ultra-strongly coupling the vibrations of the reactants to the infrared vacuum electromagnetic field. To demonstrate the possibility of such vacuum-field catalysis (or cavity catalysis), we have studied hydrolysis reactions under the vibrational ultra strong coupling (V-USC) of the OH stretching mode of water to a Fabry-Pérot microfluidic cavity mode. This results in a giant Rabi splitting energy (92 meV), indicating the system is in the V-USC regime. We have found that V-USC water enhances the hydrolysis reaction rate of cyanate ions by 10^2-fold and that of ammonia borane by 10^4-fold. This catalytic ability is found to depend upon the coupling ratio of the vibrational light-matter interaction. Given the vital importance of water for life and human activities, we expect that our finding not only offers an unconventional way of controlling chemical reactions by vacuum-field catalysis but also brings a fresh perspective to science and technology.

*Corresponding Author: Hidefumi Hiura

E-mail: h-hiura_bq@ nec.com

Tel: +81 80 8840 1581

Light-matter interactions have recently revealed an intriguing frontier for material science and chemistry[1]. In particular, it has been demonstrated that chemical reactions can be modified by coupling the reactant's vibrational transitions[2–4]. In such a case, a vibrational mode of a molecule is resonantly coupled to an optical mode of a cavity, thereby creating a pair of vibro-polaritons, i.e., light-matter hybrid (Fig. 1)[1,5]. Such vibrational strong coupling (V-SC) with an infrared (IR) electromagnetic vacuum field has been demonstrated both for solids and liquids in Fabry-Pérot (FP) cavities[1–4,6–12]. Moreover, theoretical model systems have been studied to understand how light-matter interactions affect the properties of the systems including chemical reactivity[13–17].

In sharp contrast to earlier studies where the reaction rates decreased under V-SC[2,3], an accelerated reaction under V-SC has been reported recently: an ~10-fold rate-increase was observed for the solvolysis (ethyl acetate) of para-nitrophenyl acetate under V-SC[4]. Here, for the first time, we demonstrate vacuum-field catalysis[18] (or cavity catalysis[4]) under vibrational ultra strong coupling (V-USC), showing an ~10^2-fold rate-increase for the hydrolysis (H_2O) of cyanate ions (OCN^-) and an ~10^4-fold rate-increase for the hydrolysis (H_2O) of ammonia borane (NH_3BH_3).

Figure 1 schematically outlines the vibrational light-matter coupling of water with an FP cavity. In brief, as shown in column (b), a pair of polaritonic states (P_- and P_+) emerges when the OH stretch mode of water is vibrationally coupled with a given optical mode of an FP cavity under the resonant condition of $\omega_0 = \omega_c$, where ω_0 is the fundamental vibrational frequency of the OH stretch mode, and ω_c is the frequency of the cavity mode. The difference in energy between P_+ and P_-, so-called Rabi splitting energy, is given by the following equation[1,5,6]:

$$\hbar\Omega_\mathrm{R} = 2\sqrt{N}Ed = 2\sqrt{N}\sqrt{\frac{\hbar\omega_0}{2\varepsilon_0 V}}\,\mathrm{d}\sqrt{n_\mathrm{ph}+1} \tag{1}$$

where $\hbar$ is the reduced Planck constant, N is the number of coupled molecules, E is the amplitude of the electric field of light, d is the transition dipole moment of the molecules, n_ph is the number of photons populating the cavity mode, ε_0 is the dielectric constant of vacuum, and V is the mode volume. When $n_\mathrm{ph} = 0$, $\hbar\Omega_\mathrm{R}$ has a finite value known as the vacuum Rabi splitting energy, which is due to the quantum fluctuation of IR vacuum field. The presence of such residual $\hbar\Omega_R$ is crucial for vacuum-field catalysis because it ensures that vacuum-field catalysis works as a reaction booster even without any photons[18]. In addition, like conventional catalysis, vacuum-field catalysis requires no additional energy to function as a catalyst. The coupling ratio (or coupling strength) is defined as $\Omega_R/2\omega_0$ (refs.[19,20]). The boundary between the strong and ultra-strong coupling regimes is most often drawn at $\Omega_R/2\omega_0 = 0.1$ (refs.[19,20]). Note that $\Omega_R/2\omega_0$ is a decisive factor to define the catalytic power for vacuum-field catalysis under V-SC and V-USC as shown later.

To achieve V-SC and V-USC, the FP cavity is tuned to a molecular vibration by simply adjusting the distance between the two mirrors of the cavity, namely, the cavity length (see Supplementary Information: SI 1–3). Figure 2A compares the IR spectra of light-coupled OH (OD) oscillators in H_2O (D_2O). The original OH (OD) mode is located at ω_0 = 3400 (2500) cm^{-1}. These modes are coupled to the 9th and 7th cavity modes, thereby forming pairs of vibro-polaritons P_{9+}/P_{9-} and P_{7+}/P_{7-}, respectively. The measured Ω_R is approximately 740 cm^{-1} for pure H_2O and 540 cm^{-1} for pure D_2O. The square root dependence is expected from equation (1), namely, $\Omega_R/2\omega_0 = A_c(C/C_0)^{0.5}$, where A_c is a constant equal to $\Omega_R/2\omega_0$ of the pure material. The least-squares fits (Fig. 2B) give A_c = 0.113 for H_2O and 0.111 for D_2O, confirming that the regime belongs to ultra strong coupling ($\Omega_R/2\omega_0 \geq 0.1$). Note that light-coupled water has the largest Ω_R for vibrational light-matter coupling in molecular liquid[8,21].

Next, the hydrolysis reaction under V-USC of the OH (OD) stretch of H_2O (D_2O) for the following reaction is studied:

$$2H_2O\ (2D_2O) + OCN^{-} \rightarrow CO_3^{2-} + NH_4^{+}\ (ND_4^{+})$$

where H_2O (D_2O) acts both as a reactant and a solvent for the hydrolysis of cyanate ions (OCN^-). Figures 3A and 3B present the comparisons of temporal changes in IR spectra observed for the hydrolysis of OCN^- in uncoupled H_2O (D_2O) and under V-USC at room temperature, respectively (see SI 1–4 for details). The insets of Figures 3A and 3B show that the absorption band of OCN^- stretch under V-USC decreases much faster than they do with no V-USC. Since water was present in a large excess over OCN^- in these solutions, the hydrolysis obeys a pseudo-first-order rate equation, $C = C_0 \exp(-\kappa' t)$, where C is the time-dependent concentration of OCN^-, C_0 is the initial concentration of OCN^- (2.00 $mol \cdot dm^{-3}$), κ' is the observed reaction rate constant of the hydrolysis (i.e., the product of the absolute rate constant κ and the H_2O (D_2O) concentration), and t is the reaction time. Thus, the logarithmic plot (Fig. 3C) gives a rate constant under V-USC of H_2O (D_2O), $\kappa'_- = 6.4 \times 10^{-5}$ (1.6×10^{-5}) s^{-1}, while that for the uncoupled H_2O (D_2O) is $\kappa'_0 = 5.6 \times 10^{-7}$ (5.1×10^{-7}) s^{-1}, demonstrating a 100-fold enhancement in the absolute rate constant under V-USC for H_2O and a 30-fold enhancement for D_2O. Figure 3D shows the dependence of κ'_- on Ω_R for light-coupled OH (OD) oscillators when tuned from $\Omega_R = 709$ (518) to 355 (259) cm^{-1} by diluting H_2O (D_2O) with D_2O (H_2O). κ'_- increases exponentially with an increase of Ω_R for both OH and OD light-coupled vibrations.

We next explore these accelerated reactions on the basis of a reaction kinetic model under IR vacuum field[19]. This kinetic model hypothesizes the reshape in reaction potential surface when going from the original potential to light-coupled potentials. In brief, when the Rabi splitting emerges, the force constant changes from k_0 to $k_\pm$ in accordance with the frequency change from ω_0 to $\omega_\pm$, where suffixes 0, +, and – denote the original, P_+ polariton, and P_- polariton, respectively. Because the force constant is also mechanically defined as the second derivative of the bottom of a vibrational potential, such changes in force constant reshape the corresponding reaction potential surfaces. Such reshapes in potential surface in turn alter reaction barrier heights. Among a pair of light-coupled potentials, namely, P_+ and P_- potentials, almost all the reactants proceed via the P_- potential because it has a lower activation energy than the P_+ potential.

The above kinetic model supposes that the reshape in reaction potential is driven by $\sqrt{N}$-multiplied collective quantities, IR vacuum field ($\sqrt{N}E$) or transition dipole moment ($\sqrt{N}d$), under vibrational light-matter coupling:, e.g., for the OH stretch of H_2O, equation (1) yields $\sqrt{N}E \approx 65\ \mathrm{MV \cdot cm^{-1}}$ or $\sqrt{N}d \approx 10^5\mathrm{D}$ (D: debye) when n_{ph} is zero[18]. The former value is large enough to change reaction potentials, considering that electric-field catalysts (or electrostatic catalysts) can accelerate reactions up to ~10^5 rate-increase under a static electric field of 10~140 $MV \cdot cm^{-1}$ (refs. [22,23]).

Such qualitative picture of the vacuum-field catalysis can be analytically described by using the relative reaction rate constant (κ_{-}/κ_0) as follows: by substituting next two formulae, $\omega_{\pm}/\omega_0 = (1 \pm \Omega_R/2\omega_0)$ and $E_{\pm}/E_0 = (1 \pm \Omega_R/2\omega_0)^2$, where $E_{\pm}$ is the activation energy via the $P_{\pm}$ potential under vibrational light-matter coupling and E_0 is the original activation energy, into the Eyring–Polanyi equation of the transition state theory[24,25], we obtain the following equation[18]:

$$\frac{\kappa_{\pm}}{\kappa_0} = \left(1 \pm \frac{1}{2}\frac{\Omega_R}{\omega_0}\right) \exp\left[\left(-\frac{E_0}{k_B T}\right)\left\{\left(1 \pm \frac{1}{2}\frac{\Omega_R}{\omega_0}\right)^2 - 1\right\}\right] \quad (2)$$

where $\kappa_{\pm}$ is the reaction rate constant via the $P_{\pm}$ potential under vibrational light-matter coupling, respectively, κ_0 is the original reaction rate constant, k_B is the Boltzmann constant, and T is the absolute temperature. Note that in equation (2), κ_{+} and κ_{-} correspond to the reaction rate constants for decelerated and accelerated reactions, respectively. Since all the reactions reported here are vacuum-field catalysed (rate-accelerated), we hereafter focus on κ_{-} in equation (2) with a minus sign. Equation (2) is a function of $\Omega_R/2\omega_0$, indicating that $\Omega_R/2\omega_0$ is a key parameter for vacuum-field catalysis, as mentioned earlier. As $\Omega_R/2\omega_0$ increases, κ_{-}/κ_0 increases exponentially. Note that the relation between κ'_{-} and Ω_R for light-coupled OH (OD) oscillators (Fig. 3D) can be well fitted by equation (2). Furthermore, the least-squares fitting gives $E_0 = 15.3$ kcal·mol^{-1} (0.66 eV), which agrees well with the literature value of 16 kcal·mol^{-1} (0.69 eV)[26] (see SI 1–4 for details).

In the next example, a ten-thousand-fold acceleration in the hydrolytic dehydrogenation of ammonia borane (NH_3BH_3) under V-USC of H_2O was observed and is shown in Figures 4A and 4B (see SI 1–5 for details). Equation (2) properly predicts that $\kappa_{-}/\kappa_0 = \sim 10^4$ for this hydrolysis. These results imply that the above-mentioned kinetic model is at least applicable to hydrolysis reactions under V-SC to V-USC. Further experiments of vacuum-field catalysis have demonstrated that equation (2) can account rather well for several non-aqueous reactions under V-SC (see SI 2 and 3 with Figs. S1–S6). From these results, we reckon that vacuum-field catalysis may be understood as a rate-accelerator empowered by giant IR vacuum field ($\sqrt{N}E$) or giant transition dipole moment ($\sqrt{N}d$) under vibrational light-matter coupling.

Finally, we discuss about the decelerated reactions under V-SC reported so far[2,3]. We suspect that the reactants in such a decelerated reaction may follow the P_+ potential and their rate equation may be described by equation (2) with a plus sign, in which κ_+ / κ_0 is always less than one[18]. In this scenario, the reaction path on the P_+ potential must be solely opened. However, we have no particular idea of how the path on the P_- potential is closed for such decelerated reactions. Thus, considering the myriad chemical reactions and their diverse nature, it will be necessary to compare more examples of different types of reactions in order to understand reactions under vibrational light-matter coupling.

To conclude, we anticipate that V-USC water can play a central role in vacuum-field catalysis because of the following reasons: (1) Water is of the essence in nature and in industry because it is utilized as reactants and media for numerous chemical reactions. (2) V-USC water possesses one of the largest Ω_R values among all the reactants. (3) Because water can be used as both a reactant and a solvent, V-USC water may maintain high reactivity through the endpoint of vacuum-field-catalysed reactions. Another advantage of water is that if water takes a form of microsphere in air, it may function as a self-resonator to generate a series of whispering gallery modes in an IR region. A simple estimate predicts that such airborne aqueous microdroplets can serve as a self-contained chemical reactor ideal for vacuum-field catalysis as long as the resonance condition of V-USC is fulfilled: their resonant diameters are distributed discretely but more densely than expected. To our surprise, not a few water-involved reactions have been in fact found to be dramatically promoted if confined in micrometer-sized water droplets[27,28]. The implications of such vacuum-field microreactors are as follows: what intrigues us the most is a possibility that nature might have already harnessed the principle of vacuum-field catalysis like an electric-field catalyst embedded in an enzymatic protein[22]. What if not all but a part of tiny dews of water—cloud, fog and marine aerosols—can be viewed as a naturally occurring vacuum-field reactor? Is there any chance that such a batch of microscopic "hydrospheres" have been and still are synthesising something beneficial and/or unfavourable to life and the global environment[29]? How much possibility was there that they could have played any active role in abiogenesis[30]?: how can a primordial sea mist be unrealistic, if enforced by the catalytic power of V-USC water? We envision that these pure but sound speculations will nurture a new dimension of science and technology.

References

1. Ebbesen, T. W. Hybrid light-matter states in a molecular and material science perspective. *Acc. Chem. Res.* **49**, 2403−2412 (2016).
2. Thomas, A. et al. Ground-state chemical reactivity under vibrational coupling to the vacuum electromagnetic field. *Angew. Chem. Int. Ed.* **55**, 1−6 (2016).
3. Thomas, A. et al. Tilting a ground-state reactivity landscape by vibrational strong coupling. *Science* **363**, 615–619 (2019).
4. Lather, J., Bhatt, P., Thomas, A., Ebbesen, T. W. & George, J. Cavity catalysis by cooperative vibrational strong coupling of reactant and solvent molecules. *Angew. Chem. Int. Ed.* **58**, 1–5 (2019).
5. Törmä, P. & Barnes, W. L. Strong coupling between surface plasmon polaritons and emitters: a review. *Rep. Prog. Phys.* **78**, 013901 (2014).
6. Shalabney, A. et al. Coherent coupling of molecular resonators with a microcavity mode. *Nat. Comm.* **6**, 5981 (2015).
7. Shalabney, A. et al. Enhanced Raman scattering from vibro-polariton hybrid states. *Angew. Chem. Int. Ed.* **54**, 7971−7975 (2015).
8. George, J. et al. Multiple Rabi splittings under ultrastrong vibrational coupling. *Phys. Rev. Lett.* **117**, 153601 (2016).
9. Long, J. P. & Simpkins, B. S. Coherent coupling between a molecular vibration and Fabry–Pérot optical cavity to give hybridized states in the strong coupling limit. *ACS Photonics* **2**, 130−136 (2015).
10. Dunkelberger, A. D., Spann, B. T., Fears, K. P., Simpkins, B. S. & Owrutsky, J. C. Modified relaxation dynamics and coherent energy exchange in coupled vibration-cavity polaritons. *Nat. Comm.* **7**, 13504 (2016).
11. Xiang, B. et al. Two-dimensional infrared spectroscopy of vibrational polaritons. *Proc. Natl. Acad. Sci. USA* **115**, 4845−4850 (2018).
12. Crum, V. F., Casey, S. R. & Sparks, J. R. Photon-mediated hybridization of molecular vibrational states. *Phys. Chem. Chem. Phys.* **20**, 850–857 (2018).
13. Flick, J., Ruggenthaler, M., Appel, H. & Rubio, A. Atoms and molecules in cavities, from weak to strong coupling in quantum-electrodynamics (QED) chemistry. *Proc. Natl. Acad. Sci. USA* **114**, 3026–3034 (2017).

14. Galego, J., Garcia-Vidal, F. J. & Feist, J. Many-molecule reaction triggered by a single photon in polaritonic chemistry. *Phys. Rev. Lett.* **119**, 136001 (2017).
15. Martínez-Martínez, L. A., Ribeiro, R. F., Campos-González-Angulo, J. & Yuen-Zhou, J. Can ultrastrong coupling change ground-state chemical reactions? *ACS Photonics* **5**, 167–176 (2018).
16. Galego, J., Climent, C., Garcia-Vidal, F. J. & Feist, J. Cavity Casimir-Polder forces and their effects in ground-state chemical reactivity. *Phys. Rev. X* **9**, 021057 (2019).
17. Kéna-Cohen, S. & Yuen-Zhou, J. Polariton chemistry: Action in the dark. *ACS Cent. Sci.* **5**, 386–388 (2019).
18. Hiura, H. & Shalabney, A. A reaction kinetic model for vacuum-field catalysis based on vibrational light-matter coupling. ChemRxiv. Preprint. https://doi.org/ 10.26434/chemrxiv.9275777.v1 (2019).
19. Ciuti, C. & Bastard, G. Quantum vacuum properties of the intersubband cavity polariton field. *Phys. Rev. B* **72**, 115303 (2005).
20. Bosman, S. J. et al. Multi-mode ultra-strong coupling in circuit quantum electrodynamics. *npj Quantum Information* **3**, 46 (2017).
21. Hiura, H., Shalabney, A. & George, J. Vibrational ultra strong coupling of water and ice. ChemRxiv. Preprint. https://doi.org/10.26434/chemrxiv.9808508.v1.
22. Fried, S. D., Bagchi, S. & Boxer, S. G. Extreme electric fields power catalysis in the active site of ketosteroid isomerase. *Science* **346**, 1510–1514 (2014).
23. Aragonès, A. C. et al. Electrostatic catalysis of a Diels–Alder reaction. *Nature,* **531**, 88–91 (2016).
24. Eyring, H. The activated complex in chemical reactions. *J. Chem. Phys.* **3**, 107 (1935).
25. Hänggi, P. & Talkner, P. Reaction-rate theory: fifty years after Kramers. *Rev. Mod. Phys.* **62**, 251–341 (1990).
26. Lister, M. W. Some observations on cyanic acid and cyanates. *Can. J. Chem.* **33**, 426–440 (1955).
27. Fallah-Araghi, A et al. Enhanced chemical synthesis at soft interfaces: A universal reaction-adsorption mechanism in microcompartments. *Phys. Rev. Lett.* **112**, 028301 (2014).

28. Lee, J. K., Samanta, D., Nam, H. G. & Zare, R. N. Micrometer-sized water droplets induce spontaneous reduction. *J. Am. Chem. Soc.* **141**, 10585–10589 (2019).
29. Schwartz, S. Cloud Chemistry. *Handbook of Weather, Climate, and Water.* (eds Potter, T. D. & Colman, B, R) (Wiley-Intersclence, 2003), Chap. 17, pp. 331–345.
30. Dobson, C. M., Ellison, G. B., Tuck, A. F. & Vaida V. Atmospheric aerosols as prebiotic chemical reactors. *Proc. Natl. Acad. Sci. USA* **97**, 11864–11868 (2000).

Acknowledgements

The authors acknowledge Professor Thomas W. Ebbesen for valuable discussions. H.H. thanks Jingwen Lu for assisting in the laboratory work.

Author contributions

A.S. instructed H.H. on how to perform V-SC experiments. H.H. planned the project of vacuum-field catalysis under V-USC. H.H acquired and analyzed the IR data. H.H. wrote the manuscript, and A.S. revised it. All authors contributed to discussions.

Additional information

Supplementary information is available for this paper.

Data availability

All data generated or analysed during this study are included in this published article (and its supplementary information files).

Figure 1

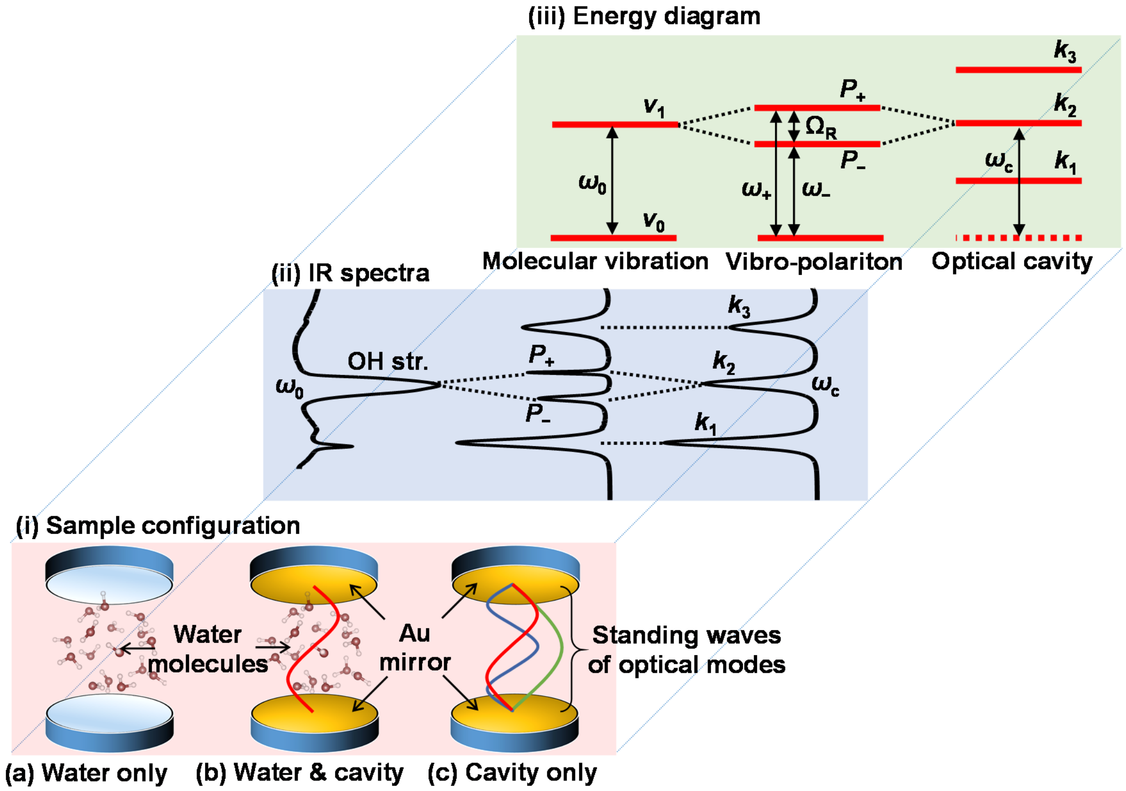

Fig. 1. Schematic overview of the vibrational light-matter coupling. The bottom, middle, and t rows show (i) sample configurations, (ii) IR transmission spectra, and (iii) energy diagrams, respectively. The left, middle, and right columns correspond to (a) water not in an FP cavity (just in an IR cell), (b) water in an FP cavity, and (c) an FP cavity without water, respectively.

Figure 2

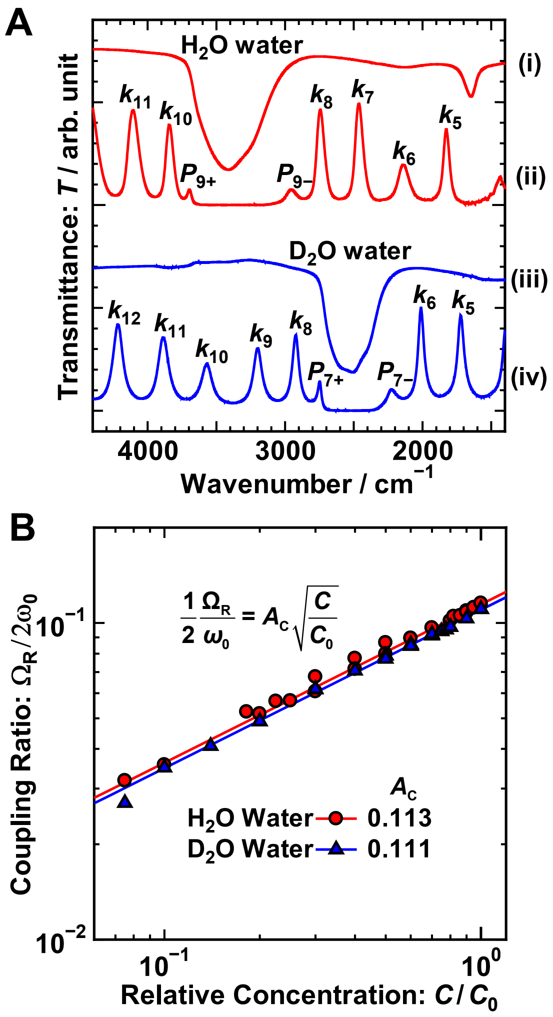

Fig. 2. V-USC of the OH (OD) stretch of H_2O (D_2O). (A) Comparison of the IR spectra of uncoupled and light-coupled H_2O (D_2O). (i) and (iii) are the IR spectra of pure H_2O and D_2O, respectively, without V-USC, whereas (ii) and (iv) are those measured with V-USC, respectively. All the spectra are normalized to unity. (B) Relation between $\Omega_R/2\omega_0$ and relative concentration (C/C_0), where C_0 denotes the concentration of pure H_2O (D_2O), namely, ~55.3 (~55.1) mol·dm^{-3}.

Figure 3

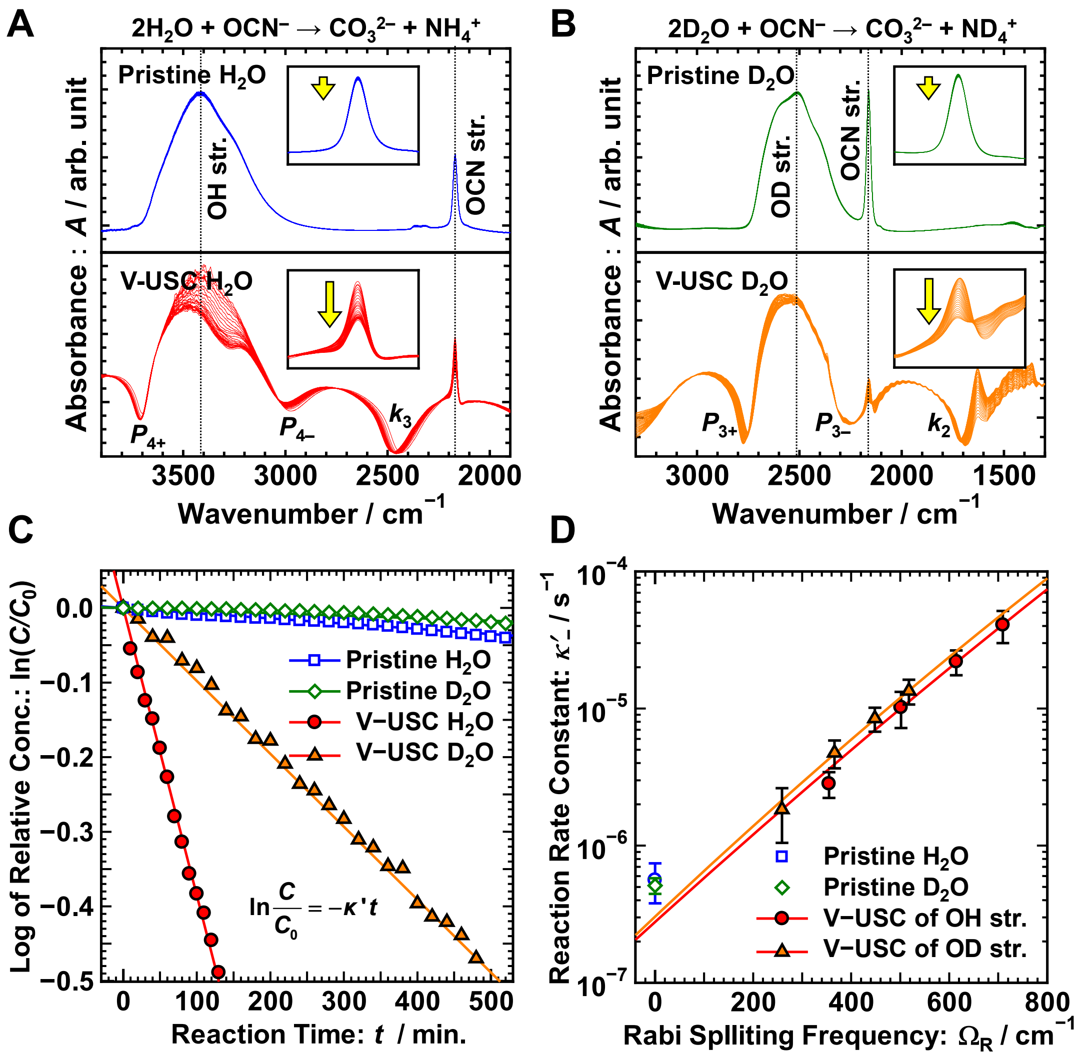

Fig. 3. Demonstration of the vacuum-field catalyst for OCN$^-$ under V-USC of water. (A) and (B) Comparison of temporal changes in IR absorption spectra observed for the hydrolysis of OCN$^-$ with pristine and V-USC H_2O, and pristine and V-USC D_2O. Insets show the magnified O=C=N stretch band during the reaction. (C) Comparison of the reaction profile for the hydrolysis of OCN$^-$. (D) κ'_- versus Ω_R on a semilogarithm scale for light-coupled OH and OD oscillators. Each bar denotes the standard errors of experimental values. The curves were drawn according to equation (2) by least-squares fitting. As a guide, κ_0 of pristine H_2O ($5.61 \pm 1.82 \times 10^{-7}$ s^{-1}) and D_2O ($5.12 \pm 0.68 \times 10^{-7}$ s^{-1}) were respectively plotted at Ω_R = 0 cm^{-1}.

Figure 4

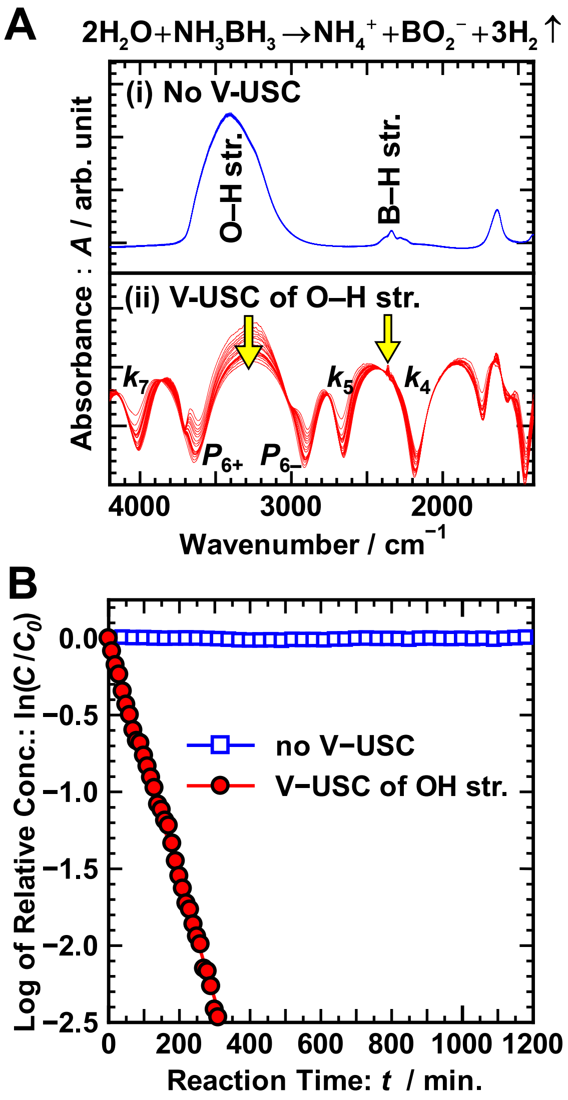

Fig. 4. Demonstration of the vacuum-field catalyst for NH_3BH_3 under V-USC of water. (A) Comparison of temporal changes of IR spectra observed for a hydrolysis of NH_3BH_3, (i) without V-USC, and (ii) with V-USC of the OH stretch. (B) Comparison of reaction profiles under the conditions of (i) and (ii). The pseudo-first-order rate constants were determined as follows: (i) $\kappa'_0 = 1.29 \times 10^{-8}$ s^{-1} (blue), and (ii) $\kappa'_- = 1.29 \times 10^{-4}$ s^{-1} (red).